doi:10.1016/j.jmb.2008.03.026 *J. Mol. Biol.* (2008) **378**, 1016–1030

JMB

Available online at www.sciencedirect.com

ScienceDirect

ELSEVIER

A Unique Mode of Microtubule Stabilization Induced by Peloruside A

J. Torin Huzil[1], John K. Chik[2], Gordon W. Slysz[2], Holly Freedman[1], Jack Tuszynski[1], Richard E. Taylor[3], Dan L. Sackett[4] and David C. Schriemer[2]*

[1]*Division of Experimental Oncology, Cross Cancer Institute, 11560 University Avenue, Edmonton, Alberta, Canada T6G 1Z2*

[2]*Department of Biochemistry and Molecular Biology, Faculty of Medicine, University of Calgary, 3330 Hospital Drive NW, Calgary, Alberta, Canada T2N 4N1*

[3]*Department of Chemistry and Biochemistry and the Walther Cancer Research Center, University of Notre Dame, 251 Nieuwland Science Hall, Notre Dame, IN 46556-5670, USA*

[4]*Laboratory of Integrative and Medical Biophysics, National Institute of Child Health and Human Development, National Institutes of Health, 9 Memorial Drive, Bethesda, MD 20892-0924, USA*

Received 11 December 2007; received in revised form 8 March 2008; accepted 11 March 2008
Available online 19 March 2008

Edited by J. E. Ladbury

Microtubules are significant therapeutic targets for the treatment of cancer, where suppression of microtubule dynamicity by drugs such as paclitaxel forms the basis of clinical efficacy. Peloruside A, a macrolide isolated from New Zealand marine sponge *Mycale hentscheli*, is a microtubule-stabilizing agent that synergizes with taxoid drugs through a unique site and is an attractive lead compound in the development of combination therapies. We report here unique allosteric properties of microtubule stabilization via peloruside A and present a structural model of the peloruside-binding site. Using a strategy involving comparative hydrogen–deuterium exchange mass spectrometry of different microtubule-stabilizing agents, we suggest that taxoid-site ligands epothilone A and docetaxel stabilize microtubules primarily through improved longitudinal interactions centered on the interdimer interface, with no observable contributions from lateral interactions between protofilaments. The mode by which peloruside A achieves microtubule stabilization also involves the interdimer interface, but includes contributions from the α/β-tubulin intradimer interface and protofilament contacts, both in the form of destabilizations. Using data-directed molecular docking simulations, we propose that peloruside A binds within a pocket on the exterior of β-tubulin at a previously unknown ligand site, rather than on α-tubulin as suggested in earlier studies.

Keywords: microtubules; peloruside A; mass spectrometry; hydrogen–deuterium exchange; simulations

Introduction

The success of taxanes in cancer treatment demonstrates the relevance of microtubules as a therapeutic target; however, numerous suboptimal pharmacological properties of these compounds have spurred the discovery and development of taxoid mimetics. While the taxoid binding site appears able to accommodate a growing variety of

*Corresponding author. E-mail address: dschriem@ucalgary.ca.

Abbreviations used: MSA, microtubule-stabilizing agent; GTP, guanosine 5′-triphosphate; HDX-MS, hydrogen–deuterium exchange mass spectrometry; LC-MS, liquid chromatography–mass spectrometry; GMPCPP, guanosine-5′-[(α,β)-methylene]triphosphate; MD, molecular dynamics.

chemical scaffolds,[1] distinct and separately addressable microtubule stabilization sites may have greater potential to overcome clinical challenges such as chemoresistivity and toxicity, in part through combination therapy[2] and reduced reliance on toxic drug solubilizers[3–5]. Peloruside A[6] and laulimalide[7] are two compounds that may offer the foundation for a new generation of therapeutics with these characteristics.

The macrolide peloruside A possesses an activity profile similar to that of the taxanes in that cells are arrested in G2/M phase and undergo apoptosis.[8] It appears to occupy a site distinct from the taxanes[9] and synergize with other microtubule-stabilizing agents (MSAs) at the level of tubulin assembly[10,11] and function in cell proliferation assays.[12] Most interestingly, peloruside A retains activity in cell lines overexpressing P-glycoprotein and in those with induced resistance to taxol and the taxoid mimic epothilone A.[9] This is also true for laulimalide.[7,13] The two compounds have been shown to compete in binding assays,[9] suggesting they bind to the same or an overlapping site.

For these ligands, the existence of a distinct binding site raises the possibility of a unique mechanism of microtubule stabilization. Typically, the α–β tubulin dimer self-assembles into a tubular arrangement of 13 head-to-tail protofilaments *in vivo*, although this number is dependent on many factors *in vitro*.[14,15] A dimeric unit binds two molecules of guanosine 5′-triphosphate (GTP), one at a non-exchangeable site between α- and β-tubulin, and the other at an exchangeable site on β-tubulin. In the assembled state, the hydrolysis of GTP at the exchangeable site introduces significant lattice strain, which manifests through stochastic depolymerizations.[16] During these events, the protofilaments peel away, most likely due to the inherent outward curvature in the dimeric unit.[17] The mechanism by which MSAs such as taxol alleviate this strain is thought to involve contributions from improved longitudinal contacts along the protofilament as well as lateral contacts between protofilaments.[18] Thus, a unique MSA binding site may alter the relative importance of these contacts and a comparative study of MSAs should shed light on the mechanisms of stabilization overall.

Much of our molecular-level understanding of MSA-induced stability has derived from cryoelectron microscopy of MSA and zinc-stabilized tubulin sheets, rather than from microtubules themselves.[18] Unfortunately, creating stable zinc sheets has not been successful for laulimalide-treated tubulin and presumably would also fail for peloruside.[19] In any case, it may be advantageous to apply a technique that can offer a differential analysis of microtubules, in both MSA-free and MSA-stabilized forms, to derive a picture of the structural impact of stabilization and identify the peloruside binding site. As an alternative to electron crystallographic data, we propose to use data from hydrogen–deuterium exchange mass spectrometry (HDX-MS). In the HDX-MS method, deuteration levels are determined from enzymatically generated peptides via liquid chromatography–mass spectrometry (LC-MS) technology.[20] This technique has been used to study protein polymers such as actin[21] and, most recently, also microtubules.[22] HDX-MS is a very sensitive probe of fluctuations in hydrogen-bonding networks, reflective of protein dynamics around a low-energy structure and commonly described in terms of "tightening" or "loosening".[23] At a minimum, this method is useful for interrogating similarities and differences in the modes of microtubule stabilization induced by different ligands.[22] Furthermore, while it is simplistic to correlate ligand-induced alterations in deuteration with a "footprint" of a binding site, it may be reasonable to expect that the footprint is at least partially represented by the ligand-altered deuteration levels. Non-covalent protein–ligand interactions are characterized by an enthalpy/entropy compensation phenomenon,[24] which can be expected to influence labelling at the binding site provided that the underlying secondary structure offers sufficient dynamic range in hydrogen-bond fluctuations. For example, HDX-MS studies of ligand-bound peroxisome proliferator-activated receptor γ have shown that the binding pocket is represented in the full set of structural stabilizations measured by the technique.[25,26] This partial correspondence has encouraged the use of HDX-MS data for scoring simulations of protein–protein interactions,[27] but this approach has not yet been applied to the discovery of binding sites for low molecular weight compounds.

In the present study, we discuss the mechanistic basis for microtubule stabilization imparted by epothilone A, docetaxel, and peloruside A. This work demonstrates a previously unknown mechanism that involves reduced reliance on lateral contacts between protofilaments. We then demonstrate a correlation between the HDX-MS data and known taxoid-site molecules (epothilone A and docetaxel), and on the basis of this evidence describe a coarse localization of the peloruside A binding site using HDX-MS data. We then apply a data-directed ligand-docking strategy to suggest a high-resolution model of the peloruside A binding site.

Results

Generation of tubulin peptide map

A map of bovine brain tubulin was generated from a pepsin digest to determine the set of peptides available for monitoring deuteration levels. Bovine tubulin contains multiple isotypes[28]; however, isotype I-C for α-tubulin and isotype II-B for β-tubulin were used to represent the map in Fig. 1. Several peptides that additionally represent other isotypes were detected. For α-tubulin, this includes two peptides for isotype αIV-A (containing the amino acids C54 and S340) and four peptides for isotype αIV-A where no corresponding peptides for αI-C are detected (containing the amino acids I122, I231-

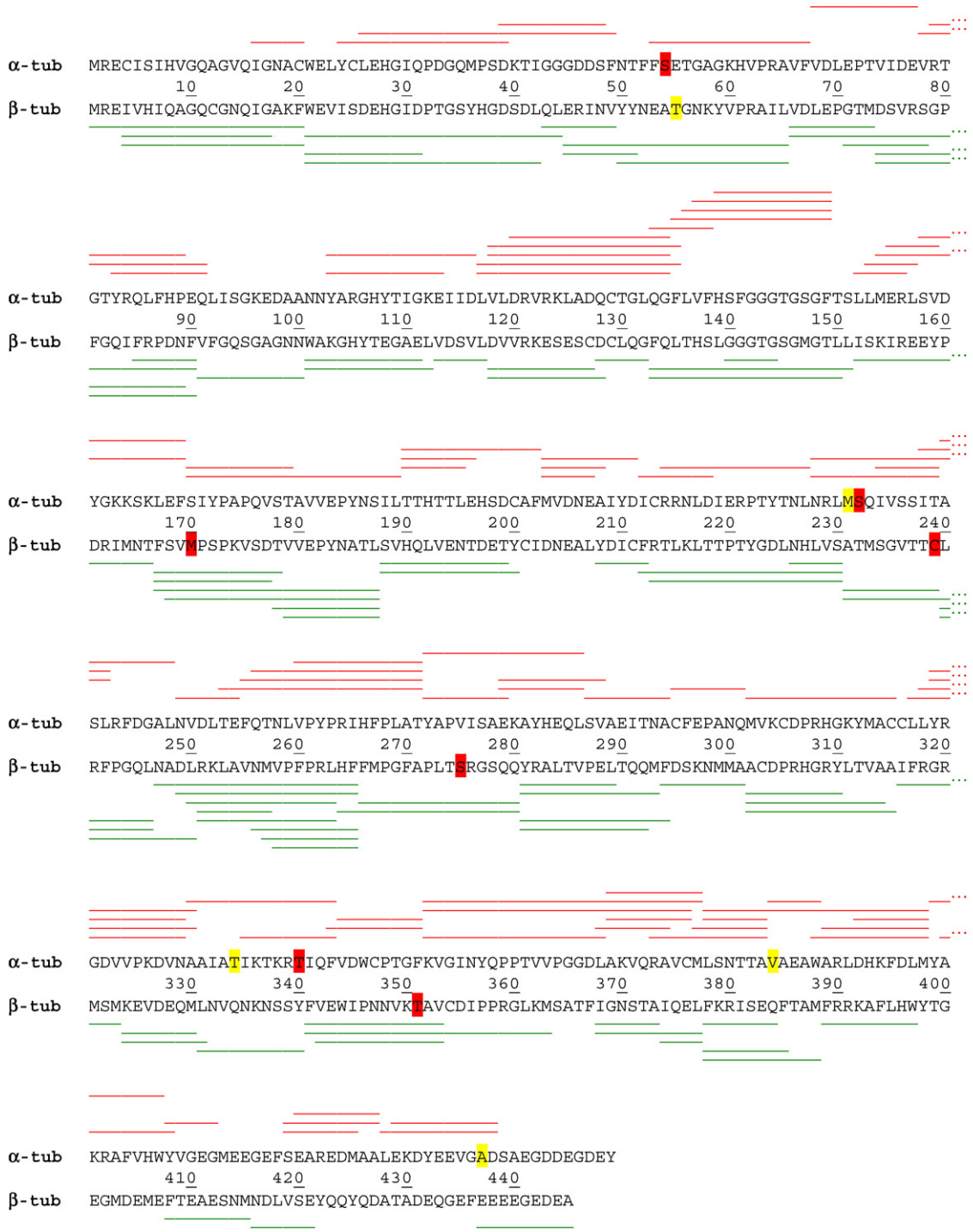

Fig. 1. Peptide map displayed in red on α-tubulin, top sequence (UniProt P81948, bovine I-C chain) and in green on β-tubulin, bottom sequence (UniProt Q6B856, bovine, II-B chain). Yellow highlighted residues represent deviations from these sequences detected in the MS/MS peptide sequence data, arising from a *different* isotype. Red highlighted residues represent the detection of an *additional* isotype in the sequence data.

S232, A34, and I384). Two other peptides represent isotype αIII (containing the amino acids G232 and V437). For β-tubulin, evidence for the presence of isotype βIII is indicated by peptides flanking the amino acids V170, S239, A275, and V351, in addition to the corresponding peptides for βII-B. A single peptide with no correspondence to βII-B contains A55, which is of unspecified bovine sequence but equivalent to porcine β-tubulin (UniProt P02554). Overall, 84 non-redundant peptides for α-tubulin were identified, leading to a sequence coverage of 88.4% and 86 non-redundant peptides for β-tubulin for a sequence coverage of 92% (inclusive of all isotypes).

One advantage of the MS-based analysis is that selective detection of isotypes is possible. As an

example, isotype βII bears a serine at position 275 in the M-loop critical to taxane binding, whereas isotype βIII has an alanine in this position (Fig. 1). The MS data show equivalent, strong reductions in labelling for the peptides that span this position. Therefore, in the context of the mixed isotype preparation, isotype βIII appears to bind both taxoid-site ligands as well as isotype βII. No cases of isotype-specific labelling were found in our study for the set of unique peptides found, and as with the published structural studies, the data for peptides common to all isotypes are most appropriately viewed as averaging any potential isotype-specific contributions to drug-induced stability.

Guanosine-5′-[(α,β)-methylene]triphosphate-stabilized bovine brain microtubules as a model system

It has been recognized that the isotype diversity of bovine brain tubulin preparations differ from that of humans, particularly in non-neuronal cells.[28] Much of the sequence difference is relegated to the C-termini of the α and β-tubulin and not in regions critical to the taxoid binding site or to assembly in general, although the kinetics of dynamic instability are isotype dependent.[29] As most of the existing experimental structural studies have been conducted on tubulin isolated from bovine brain, we chose to do the same, recognizing that bovine brain tubulin preserves 1:1 binding stochiometry (dimer:drug) irrespective of isotypes.[30]

To promote a comparison of the assembled state with ligand-stabilized microtubules we used the GTP analog guanosine-5′-[(α,β)-methylene]triphosphate (GMPCPP) at the exchangeable nucleotide binding site within β-tubulin. GMPCPP is a GTP analogue that promotes stability of the resulting microtubule by reducing the rate of nucleotide hydrolysis.[17,31,32] As the source of microtubule instability arises from nucleotide hydrolysis at this site, incorporating a slowly hydrolyzed form leads to a preparation that does not exhibit dynamic instability.[31] This is critical for differential studies, as unassembled pools of free α–β dimer will exist in GTP-loaded microtubules. Upon the addition of stabilizers, this pool will diminish in concentration, in which case the HDX-MS results will be strongly influenced by the exchange properties of the free dimer. A recent study with chicken erythrocyte tubulin has suggested that there are few labelling differences between free dimer and GTP microtubules.[22] It is possible that assembly dynamics are different for these two model systems, although we note that the Xiao *et al.*[22] study involved dilution of GTP microtubules during deuteration to below the critical assembly concentration. This may offer an alternative explanation as to why few differences between free dimer and GTP microtubules were found. In the current study, we have shown that free dimer concentrations are not detectable in either the GMPCPP microtubule or the drug-saturated states (see below).

Equilibrium deuterium exchange of ligand-free and ligand-treated microtubules

To determine an appropriate deuterium-labelling time for conducting the HDX-MS analysis, equilibrium deuterium in-exchange experiments[33] were initiated with the addition of D_2O to ligand-free microtubule preparations, and sampled over multiple time points for HDX-MS analysis (see Materials and Methods). Deuterium levels reached a plateau at 8 min of labelling time, representing ~20% deuterium incorporation (uncorrected for back-exchange). Experiments were then conducted at 4 min, where 90% of the plateau-level deuteration was retained, to ensure that rapidly exchanging regions retain sensitivity as structural probes of binding. As determination of the absolute value of deuteration is not required for comparative binding studies, all deuterium levels are uncorrected for back-exchange.[34]

Equilibrium deuterium in-exchange experiments were conducted for each microtubule state using the non-liganded microtubule as a control, and average deuterium incorporation was measured using software developed in-house. The data set can be found in Supplementary Table 1a and b. A subset of the exchange data (Fig. 2a and b) represents all peptides bearing a significant difference between *one or more* ligand-stabilized microtubule preparations and the microtubule control (a ligand-free preparation). This subset of data was used in subsequent structural representations (Figs. 3–6, 8). To avoid the complexity of mixed states evident in earlier studies,[22] all microtubule preparations were generated with GMPCPP. Ligand-free microtubules were prepared well above critical concentrations for assembly and the absence of contaminating free dimer was confirmed by monitoring peptides exhibiting large reductions in deuterium labelling upon assembly, but no further reductions upon ligand binding at the same tubulin concentration. As an example, β74–89 experiences a reduction of 788±50 millimass units (mmu) upon assembly (i.e., dimer to GMPCPP-stabilized microtubules) and no further significant reduction upon docetaxel labelling (Fig. 2b). This indicates full assembly has occurred, as docetaxel leads to a significant decrease in the critical concentration of assembly.[35] Thus, ligand binding does not significantly alter the population of free *versus* assembled dimer.

Mapping the HDX-MS data

Global view

The significant differences in labelling between GMPCPP microtubules and the drug-bound forms were mapped onto representative tubulin structures to indicate regions of decreased labelling (red) or increased labelling (blue) due to ligand binding, and displayed globally in Fig. 3a–c. Graduating the degree of altered labelling via color coding was not implemented, for clarity. The taxoid-site ligands generate reductions in labelling clustered at the

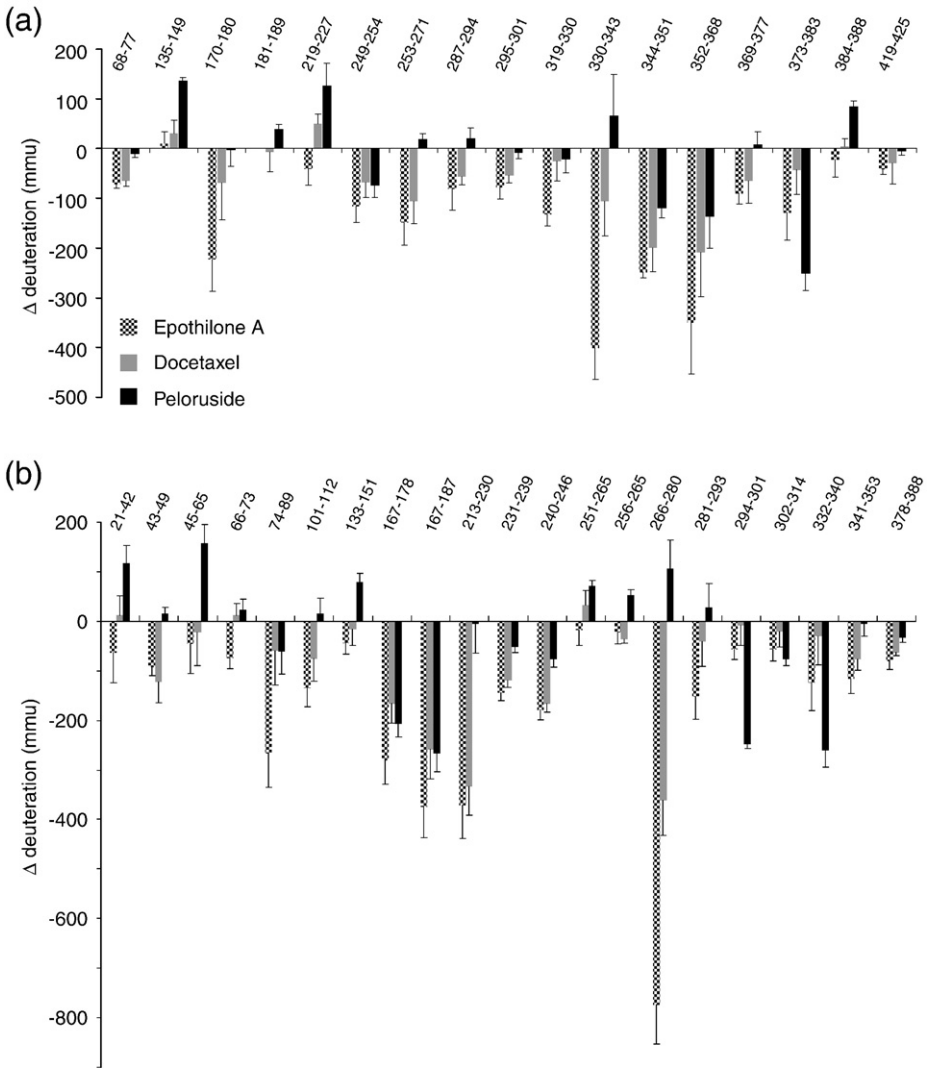

Fig. 2. Ligand-induced alterations in deuteration referenced against GMPCPP-stabilized microtubules for (a) α-tubulin (b) β-tubulin. Data indicate the mean ± pooled standard deviation of three separate experiments. Peptide sequence numberings are based on UniProt entries P81948 (α-tubulin) and Q6B856 (β-tubulin) as in Fig. 1. Altered deuteration levels are expressed in millimass units (mmu).

interfacial regions defined by the longitudinal protofilament axis of the microtubule, as well as the taxoid site itself. The effects observed for docetaxel are largely a subset of those generated by epothilone A, whereas the map for peloruside A shows considerable differences. While many of the changes cluster in the same longitudinal regions, there are significant destabilizations at the intradimer interface and at putative lateral contacts between protofilaments. Additionally, there is a mapped region of reduced labelling on the exterior of β-tubulin that is unique to peloruside A. These will be presented in greater detail.

Interdimer region

Figure 4a–c represents the subset of exchange data in the vicinity of the interdimer interface, that is, between adjacent α–β dimers on the protofilament axis of microtubules. Secondary-structure designations are made on the basis of the map in Löwe *et al.*[18] Epothilone A extensively reduces exchange dynamics at this interface, as evidenced by six peptides on α and five peptides on β tubulin (Fig. 4a). The impact of docetaxel on this region appears less strong (Fig. 4b); however, the peptides with significant labelling differences are a subset of those highlighted by epothilone A and a number of common peptides not labelled for docetaxel generate reductions just below the chosen threshold for significance (Fig. 2). Reduced labelling at this interface is also true for peloruside A, with one exception on β-tubulin (Fig. 4c). Peptide β133–151 undergoes an increase in labelling upon peloruside binding and is immediately adjacent to the nucleotide phosphates of GMPCPP. Overall, the alterations in labelling at the interdimer interface represent the largest changes not directly associated with the taxoid site, particularly for peptides on both α and β in contact with the exchangeable nucleotide (see Discussion).

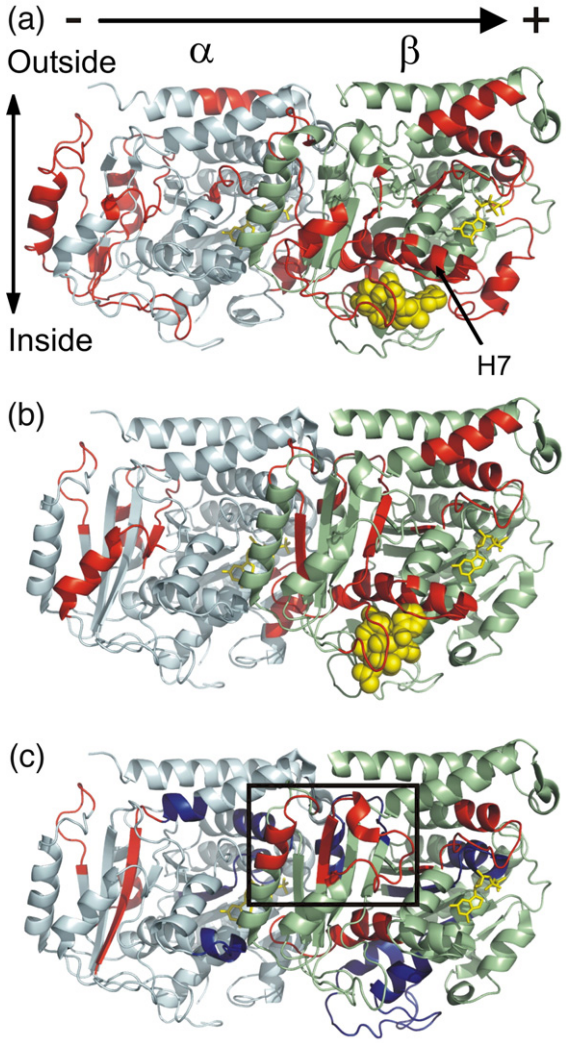

Fig. 3. Global mapping of the ligand-induced alterations in deuteration onto α-β-tubulin oriented as in a microtubule, with polarity indicated. (a) Epothilone-A-induced changes modeled on PDB 1TVK, (b) docetaxel-induced changes modeled on PDB 1JFF, and (c) peloruside-A-induced changes modeled on PDB 1JFF. Red indicates statistically significant reductions in labelling upon binding; blue indicates statistically significant increases in labelling upon binding (see Materials and Methods). Tubulin monomers are labeled in pale cyan (α) and pale green (β). The exchangeable (β-tubulin) and non-exchangeable nucleotides (α-tubulin) are labelled in yellow, and ligands in yellow spheres. The rectangle highlights the proposed peloruside A binding site, which can be found at higher magnification in Fig. 8.

Intradimer region

Figures 5a and b represent a comparison view of the α–β intradimer region centered on the non-exchangeable GTP binding site. As the changes for docetaxel are again a subset of those induced by epothilone A, only the map of the latter is shown relative to peloruside A. All ligands reduce labelling for peptides β231–239 and β240–246, but the magnitude of change is significantly lower for peloruside A (Fig. 2b). These peptides represent the H7–H8 loop (β240–246) and the C-terminal end of H7 (β231–239). The latter peptide is part of the known taxoid site.[18] While these changes are common to all three ligands, there are notable reductions in labelling that are unique to the taxoid-site ligands. Across the intradimer interface on α-tubulin, reduced dynamics are in evidence for peptides encompassing the non-exchangeable nucleotide, specifically the sugar-binding T5 loop (α170–180). Other peptides involved in stabilization of the intradimer region are also reduced in labelling (α68–77 and β341–353). Peloruside A induces a significantly different effect, where the non-exchangeable nucleotide site undergoes an increase in labelling centered on the regions adjacent to the nucleotide phosphates and involved in stabilization of the intradimer contact.[18] This includes the T4 loop (α135–149), H5 loop (α181–189), and the H8 loop (β251–265).

Mapping the HDX-MS data for lateral contacts

Lateral interactions between protofilaments are thought to be mediated by contacts between the M-

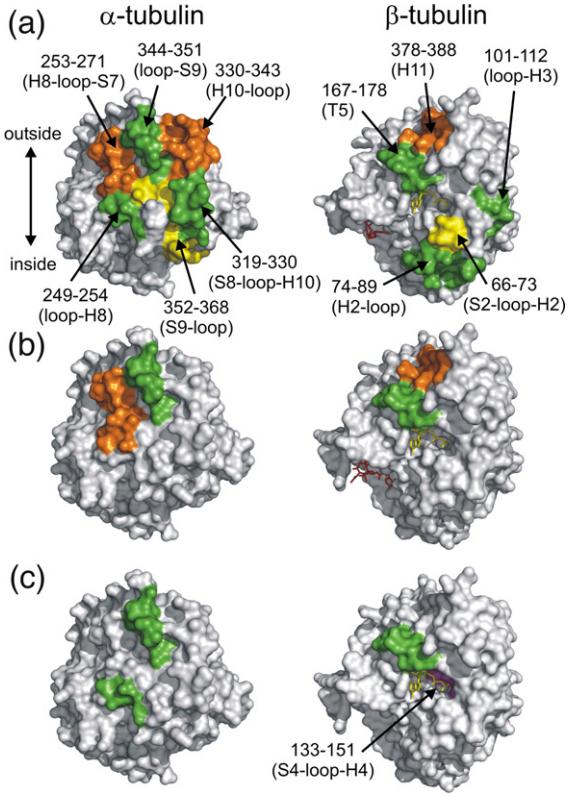

Fig. 4. Opposing views of the interdimer interface showing peptides in this region altered in deuteration level as a result of ligand binding. All other affected peptides are removed for clarity. Reductions in deuterium labelling shown in orange/green/yellow to delineate detected peptides, not degree of labelling. The increase in deuterium labelling is in magenta. The color scheme is retained for all ligands, to promote comparison among (a) epothilone A, (b) docetaxel, (c) peloruside A. The exchangeable nucleotide is displayed in yellow and ligands in red. Orientation is ±90° in the horizontal relative to Fig. 3.

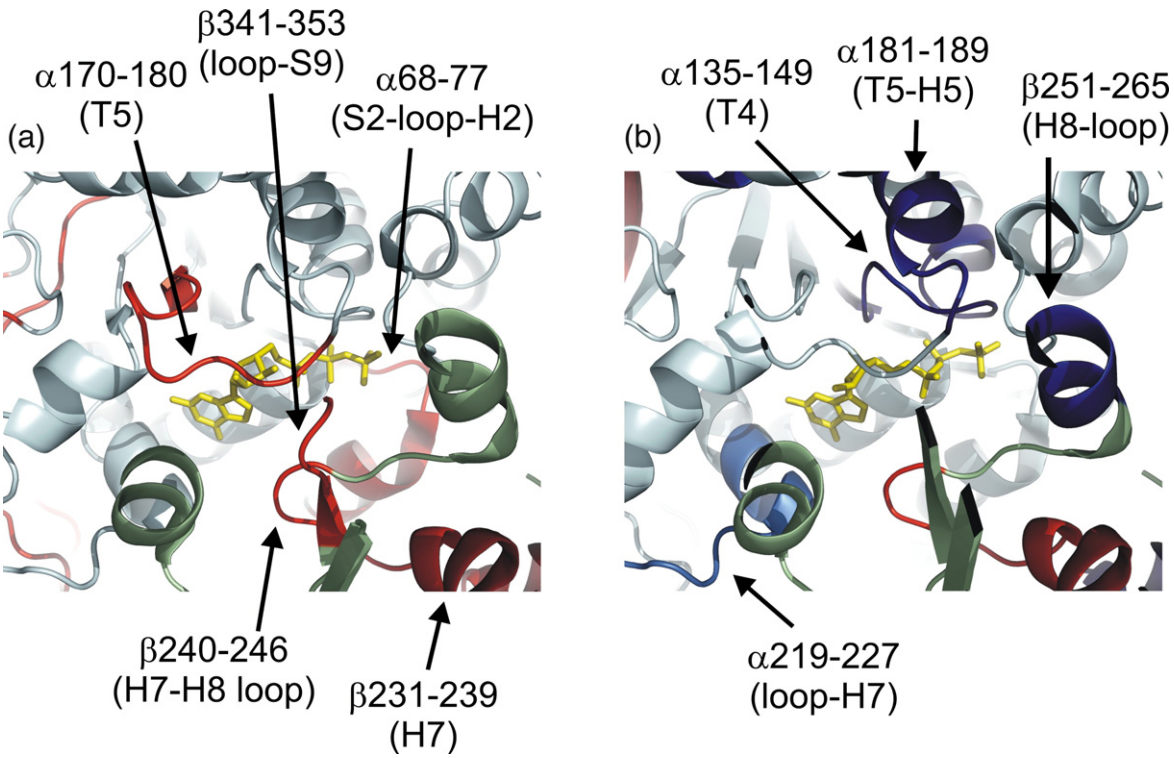

Fig. 5. Expanded view at the non-exchangeable nucleotide intradimer interface for microtubules stabilized on (a) epothilone A (on 1TVK) and (b) peloruside A (on 1JFF). Ligand-induced alterations in deuterium labelling are mapped in red (reduction), blue (increase), and light blue (increase, near global significance threshold). Other aspects of the color scheme are as in Fig. 3.

loops on α- and β-tubulin with the corresponding H1–S2 loops on the adjacent α- and β-tubulin.[36] Both taxoid-site ligands reduce labelling at the M-loop on β-tubulin, but no changes are found for the corresponding H1–S2 loops, and no changes are observed for α-tubulin. Peloruside A induces an *increase* in labelling in both the H1–S2 loop and the M-loop on β-tubulin; although the latter is just outside the defined significance level (see Fig. 2b, peptide β266–280), it is supported by an overlapping peptide (see Supplementary Table 1b). As with the taxoid-site ligands, however, no changes

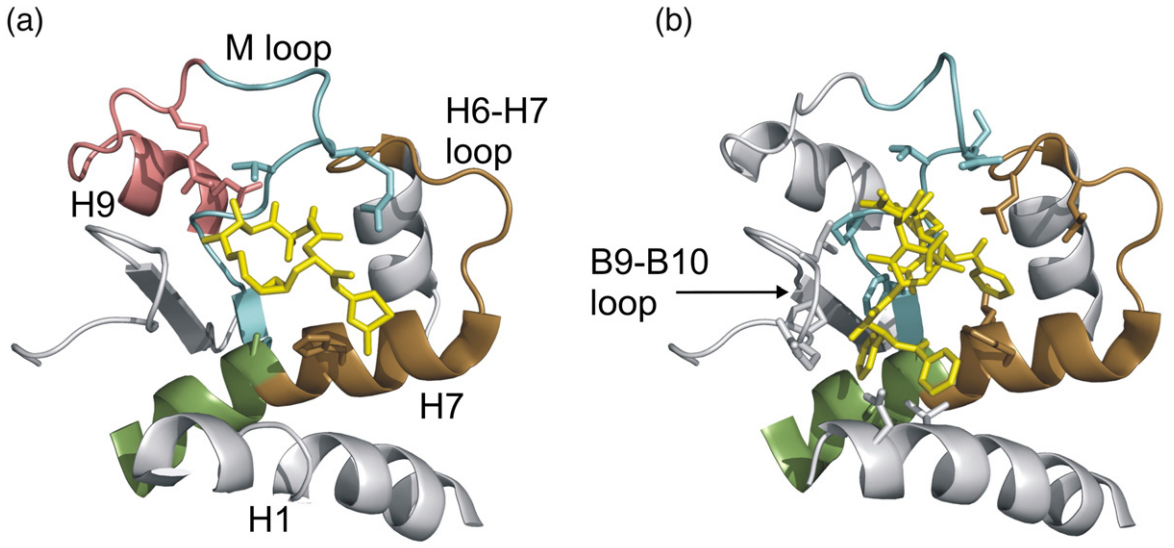

Fig. 6. Expanded view of the taxoid-binding site overlaid with labelling data. (a) Epothilone A and (b) taxol in lieu of docetaxel. Individual peptides showing reduced labelling displayed in color and corresponding secondary structure indicated (see Table 1).

Table 1. Correspondence between measured reductions in deuterium labelling and residues participating in the stabilization of the ligand–tubulin binding site

Peptic peptide[a]	Reduction in labelling (docetaxel/epothilone)	Key residues in ligand binding[b]	
		Taxol[c]	Epothilone
β21–31 (H1)	No/no	Val21	—
		Asp24	—
β213–230	Yes/yes	Leu215	—
(H6–H7 loop)		Leu217	—
β226–230 (H7)	No/no	His227	His227
		Leu228	—
β231–239 (H7)	Yes/yes	Ala231	Ala231
		Ser234	—
β266–280	Yes/yes	Phe270	—
(S7–M-loop)		Pro272	—
		Leu273	—
		Thr274	Thr274
		Ser275	—
		Arg276	Arg276
β281–293	No/yes	—	Arg282
(loop–H9)		—	Gln292
β341–363	No/no	Pro358	—
(S9–S10)		Arg359	—
		Gly360	—
		Leu361	—

[a] Secondary structure as in Lowe *et al.*[18] Residue numbering based on Fig. 1.
[b] Dash indicates no known participation in binding.
[c] Structural data derived from the taxol–tubulin structure 1JFF.

are observed in the proposed α–α lateral contact region.

Mapping the HDX-MS data to the binding sites

For both epothilone A and docetaxel, the largest reduction in labelling in the data set is found at the M-loop (β266–280). A second large reduction is found at the H6–H7 loop region (β213–230) with smaller changes at the core helix βH7 (β231–239) previously mentioned in the context of the intradimer interface. In addition to these changes, epothilone A induces a small reduction in labelling for loop H9 (β281–293). Figures 6a and b show the labelling data associated with the known taxoid-site ligands. These peptides encompass many of the key residues involved in the binding to both epothilone A and the taxanes (see Table 1). The M-loop undergoes strong reductions in labelling and brackets critical residues in the stabilization of the oxetane ring of the taxanes.[18] Identifying H7 as part of the binding site is principally through β231–239, which encompasses residues for the stabilization of the 3′-phenyl ring. The N-terminal end of H7 does not show a significant reduction in labelling (peptide β236–230, data not shown), even though this peptide contains a residue critical for the stabilization of the 2-phenyl ring. Thus, although there is a peptide that bridges this region (β213–230), the associated reduction in deuteration is due to the H6–H7 loop (β213–225). Together with βH7, this loop has been shown to stabilize the 2-phenyl ring.[18] A further underreporting of helical regions involved in binding may occur at H1 (β10–25). Residues that are involved in the stabilization of the 3′-phenyl ring as well as the *N*′-phenyl for taxol (*t*-butyl for docetaxel) are found in this helix. Surprisingly, the loop between βS9 and βS10 does not show significant labelling, even though close contact is made with docetaxel. This may be due in part to the lower resolution of the HDX-MS data for this region (a single 22-amino-acid peptide encompasses this loop). A 2.5 times greater reduction in labelling for docetaxel over epothilone A is noted for this peptide, but the error in the measurement prevents a claim of significance. The participation of P358 in the actual ligand-binding site could also reduce the ability of this region to report alteration in labelling, as prolines contain no readily exchangeable amide hydrogen. Epothilone A similarly engages residues within the M-loop and H7 helix (Table 1). The direct participation of residues in the H6–H7 loop in the binding site is less clear,[1] but reduced dynamics of H7 could stabilize this loop and promote interactions through space with the stabilized M–loop.

Clustering most of the remaining significant reductions in labelling due to peloruside A binding leads to the formation of a patch on the exterior surface of β-tubulin, composed of peptides β294–301 (H9–H9′ loop), β302–314 (H9′–S8), and β332–340 (H10 loop). With the exception of peptide β302–314, these are large reductions in deuteration, similar to what was observed for docetaxel binding. This represents a strong candidate region for the peloruside A binding site (encircled in Fig. 3c), which was further explored through docking studies.

Data-independent and data-driven docking of peloruside

We conducted molecular docking using a global search using the previously determined bound conformation of peloruside[37] and a reconstruction of an α–β–α protofilament based on PDB entry 1TVK. Using blind docking, three sites of comparable docking energies were discovered: the α-tubulin site proposed by Jimenez-Barbero *et al.*,[37] the β-tubulin site described in this study, and a site bridging the interdimer interface. As the α-tubulin site was not represented in the HDX data, it was not considered for refined docking studies. A second partially restricted docking exercise was conducted on what is the exterior face of an α–β–α protofilament segment (i.e., minus the lumenal surface). In this run, the candidate peloruside binding site on β-tubulin was identified from five distinct clusters consisting of 169 poses (based on a total of 500 poses), with 82 representing docking energies below −10 kcal/mol (Fig. 7a). A site within the interdimer interface was identified from four distinct clusters containing a total of 106 poses with 58 representing docking energies below −10 kcal/mol. As no other sites were uncovered within the regions encompassing the footprinting data, a final refined docking exercise was restricted to only these regions. For the candidate β-tubulin site, 64 of 200 poses presented

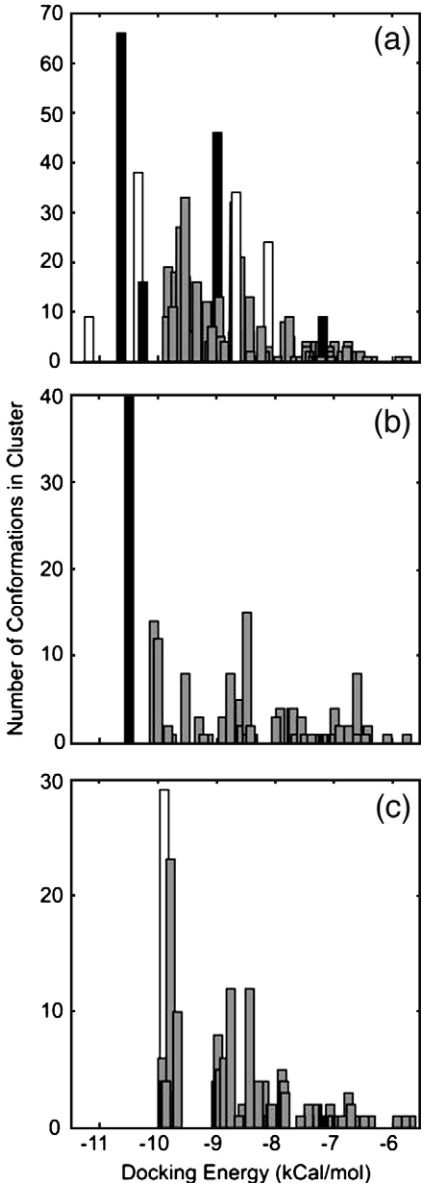

Fig. 7. Histogram of docking energies returned from the ligand-docking simulations, using the coordinates for bound peloruside and 1TVK. (a) Results from a blind docking exercise targeting the exterior surface of an α–β–α protofilament with clustering of poses at the 5 Å level, where black represents poses within the region defined by the HDX data at the β-tubulin site, white the region defined by the interdimer site, and gray the binding poses outside of the regions indicated by the HDX data. (b) Results from the directed docking to the general region of the exterior of β-tubulin with clustering of poses at the 2 Å level, where black represents the pose displayed in Fig. 8 and gray, alternative poses within or around site identified by HDX data. (c) Results from the directed docking to the general region of the exterior of the α–β interface with clustering of poses at the 2 Å level where white represents the best fit to the HDX data and gray, alternative poses within the interfacial region.

with docking energies of −10 kcal/mol or better (Fig. 7b), with 40 of these poses clustering within 2 Å of the orientation displayed in Fig. 8. For the interdimer site, 29 of 200 poses presented with a docking energy of −9.6 kcal/mol (Fig. 7c).

Molecular dynamics for binding energy estimation

Molecular dynamics (MD) simulations were then conducted for peloruside within the β-tubulin and the interdimer sites, using the low-energy docked poses as initial conformations (see Materials and Methods). For the β-tubulin site, binding energies fell between −21 and −37 kcal/mol, depending on the particular binding pose or solvation model that was implemented, and suggesting a preference for association with β294–301. For the interdimer site, binding energies fell between −13 and −32 kcal/mol, also depending on the pose and solvation model used.

Discussion

MSAs stabilize protofilaments at the interdimer interface

Stabilization of the interdimer interface appears to be a hallmark of ligand-induced microtubule stabilization, and aside from changes at the actual binding site, the greatest reductions in exchange are found in this region (Fig. 4a–c). Although the extent of reduced labelling is ligand dependent, it appears to center on β167–178 for all three MSAs investigated, which straddles the T5 loop immediately adjacent to the ribose of the exchangeable nucleotide. The taxoid-site ligands likely induce this perturbation

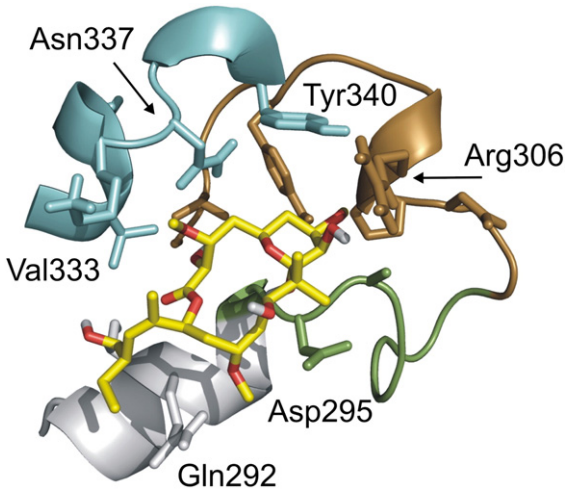

Fig. 8. Proposed peloruside A binding site as determined by combination of labelling data and local docking simulations. Individual peptides detected by HDX-MS are indicated in color (green: β294–301, H9–H9′ loop; brown: β302–314, H9′–S8; cyan: β332–340, H10 loop). Helix H9 is in gray (β286–293). Select side chains suggested to be significant in defining the binding pocket are labeled. Oxygen atoms of peloruside A are colored in red.

through the action of the core helix βH7.[38,39] This helix comprises the bottom of the cleft defining the taxoid binding site (Fig. 6a and b), and site occupancy may reduce the dynamics of H7 to affect the adjacent T5 loop and the corresponding peptide α344–351 across the interface. This latter peptide is also stabilized by all three ligands. If interdimer stabilization is indeed a primary feature of all MSAs, it is obvious this can be induced in different ways, as βH7 is largely unaffected by peloruside A (Fig. 3c). The most likely source of this perturbation arises from the proposed binding site for peloruside A on the exterior of β-tubulin, specifically peptides β294–301 and β302–314 (Fig. 8). These peptides compose the H9–S8 loop that is also adjacent to the T5 loop. Thus, we suggest that there are at least two routes to the stabilization of the T5 loop: through helix H7 and through the H9–S8 loop. MSAs induce a conformational change in the T5 loop of β-tubulin and promote improved interactions across the interdimer interface, returning a stability to the interface that may be lost upon nucleotide hydrolysis. Such an effect would be consistent with our understanding of stability in the dimer itself, where the T5 loop of α-tubulin participates in extensive monomer–monomer contacts.[18]

It is interesting to note a subtle difference between between peloruside A and the taxoid-site ligands in this region. The extensive reduction in exchange for the T5 loop seen with this peloruside A is accompanied by an increase in the exchange dynamics of the peptide adjacent to the nucleotide phosphates. This suggests that the nucleotide-binding site has become strained under the action of the T5 conformational change, perhaps indicating poorer binding of the nucleotide. Whether the increased flexibility in this region is due to the partial incompatibility of the methylene bridge of GMPCPP is not known at this time.

MSAs exert a differential effect on protofilaments at the intradimer interface

At the intradimer region, there is a significant departure between the taxoid-site ligands and peloruside A. As shown in Fig. 5, epothilone A and docetaxel reduce the exchange dynamics around the non-exchangeable GTP, but peloruside generates an increase. Both taxoid-site ligands act upon βH7 through His227 in a manner that may "lock" the H7–H8 loop at the intradimer interface and stabilize the βT5 loop as described above. Across the intradimer interface, we observe a corresponding reduction in exchange for the αT5 loop (peptide α170–180). As in β-tubulin, this loop encompasses the nucleotide ribose, and thus it appears that βH7 communicates reduced dynamics to both interfaces along the longitudinal protofilament axis. It should be stressed that the magnitude of labelling changes at the intradimer interface is generally lower than seen at the interdimer interface, suggesting that drug binding exerts a greater influence at the latter. In general, epothilone A induces greater changes than docetaxel at both interfaces. This is interesting given the similarities in free energy of binding for these two ligands[35] and that saturating levels of ligand were applied. It may be that a marked difference in binding energy between these ligands and the various tubulin isotypes is occurring leading to unequal binding-site occupancy. However, the magnitude of this difference would have to be great given that saturating ligand levels are used, and thus this argument does not seem reasonable. The greater stabilization induced by epothilone A appears to correlate with enthalpy of binding.[35] Further studies are under way to explore the relationships between hydrogen–deuterium exchange properties and MSA thermodynamic properties.

In the case of peloruside A, the C-terminal end of H7 (β231–239) and the H7–H8 loop (β240–246) experience reduced labelling in common with epothilone A and docetaxel, but to a lesser extent (Fig. 2b). This degree of stabilization is insufficient to induce the associated stabilization of the αT5 loop seen with the taxoid-site ligands. In the absence of such stabilization, the intradimer interface becomes more labelled around the non-exchangeable nucleotide phosphates at loops T4 and T5, and likely also the base (Fig. 5b; peptide α219–227 at loop H7 shows an increase just outside of the stated significance threshold). Whether this is directly through the action of an adjacent peloruside-binding site or indirectly through a stabilized interdimer interface is unclear; however, it suggests a significant departure in stability mechanisms, discussed below.

Peloruside preferentially destabilizes lateral protofilament contacts

A second region of significant destabilization accompanies peloruside A binding. An increase in labelling is found at the N-terminal H1–S2 loop (β21–42, β45–65) at the proposed lateral contact between protofilaments.[18] A similar effect on the corresponding M-loop of the adjacent β-tubulin might be expected, and indeed a change of similar magnitude is in evidence (β266–280), although the difference is also just outside of our defined significance level. However, peloruside binding returns the deuteration of this peptide to a level equivalent to that of the free dimer (data not shown) and thus is likely significant. This observation can be explained as a reduced interaction between protofilaments and strongly suggests peloruside A reduces dependency on lateral contacts for microtubule stabilization, at least between β-tubulin monomers. Interestingly, neither taxoid-site ligand affects the exchange properties of the proposed lateral contacts, suggesting that stability may be an exclusively longitudinal phenomenon under the action of these ligands.[17] This is in contrast to the findings of Xiao *et al.*,[22] who demonstrate that taxol binding stabilizes the lateral interaction at α-tubulin but not at β-tubulin. As taxol defines a microtubule with 12 protofilaments

as opposed to 13 for docetaxel,[40] this difference may reflect an alternative lattice configuration, but it could also represent an artefact arising from the presence of free dimer.

Proposed models for ligand-induced stabilization

On the basis of these findings, we suggest that an improved interdimer interaction is the primary mode of microtubule stabilization and that at least two distinct conformational responses to interdimer stabilization accompany MSA binding. In one, all longitudinal contacts are stabilized with no obvious improvement in lateral contacts. This is exemplified by the taxoid-site ligands used in this study. In the other, for peloruside A, the assembled dimer appears to adopt a configuration with greater flexibility at the intradimer interface and reduced interactions between protofilaments at β-tubulin. This may be driven by an alternative organization at the interdimer interface or possibly the absence of a stabilized βH7. Both conformational responses clearly have the potential to counteract the natural curvature of the protofilament that is the primary source of lattice strain in the assembled form.[41] It is interesting to speculate on the nature of the structural perturbation that may accompany the altered labelling described for these ligands. The taxoid-site compounds could favor a simple "tightening" along the protofilament axis, whereas peloruside A may be described by a "plate tectonic" model. In the latter, a discontinuity in the protofilament at the intradimer interface could expose regions of this interface to improved solvent exchange while still promoting strengthened interactions at the interdimer interface. Such an effect rationalizes the increased labelling between β-tubulin across protofilaments, particularly if β-tubulin moves in the lumenal direction. This model might be expected to induce a compression in α-tubulin; we note a large reduction in labelling at α373–383 for the internal beta sheet S10 (Figs. 2a and 3c), which may be evidence of this.

Labelling data encompass critical features of the taxoid site

To precisely identify the peloruside A binding site, it is useful to first consider the congruence between the exchange data and the known taxoid site for epothilone A and docetaxel. There is general agreement between the HDX data and the known binding sites for these ligands (see Table 1 and Fig. 6a and b). Indeed, the sensitivity of the HDX data to site stabilization can be seen when comparing the results for epothilone A with docetaxel in the vicinity of the M-loop. Based on the epothilone A–tubulin structure 1TVK, Q292 of helix H9 participates in the stabilization of the M-loop through hydrogen bonding,[42] and a segment spanning this residue and the C-terminal region of the M-loop undergoes a reduction in labelling. Q292 does not participate in the docetaxel-induced stabilization, and no HDX labelling changes are observed (Fig. 6b). Although not all residues critical to ligand binding are revealed in the data, this may be expected because binding will not distort hydrogen bonding in a universal manner. For example, the N-terminal end of βH7 is "silent" most probably because internal hydrogen bonding is little influenced by ligand binding. Overall, it is clear that such data may be used to identify binding sites for other MSAs.

Data-directed ligand docking suggests a novel peloruside A binding site

A strong candidate binding site for peloruside A is the region of reduced labelling on the exterior of β-tubulin (Fig. 3c), as mapped by peptides β294–301 (H9–H9′ loop), β302–314 (H9′–S8), and β332–340 (H10 loop). To test this location as the peloruside-binding site and generate a high-resolution ligand-binding model, we implemented both blind and data-directed docking simulations. Blind binding site predictions using tools such as AutoDock have been implemented on several systems,[43,44] including tubulin.[38] However, application of a blind docking exercise using the known conformation of bound peloruside was insufficient to identify the binding site with high confidence (Fig. 7a). The precision of these simulations increases when transitioning from blind to data-led docking. In these experiments, docking simulations were focused on grids fully encompassing labelling data for the proposed binding site, as well as the exterior surface flanking the interdimer interface. The interdimer region was added, since upon assembly of an α–β–α protofilament model, a surface map of the labelling data suggested the possibility of a contiguous region bridging this interface (not shown). These directed docking experiments allowed extensive sampling of local regions of the microtubule surface and improved discrimination between poses. The simulations (Fig. 7b) support peloruside A binding at the β-site as localized by the labelling data and provide a high-resolution binding model of peloruside within the site (Fig. 8). Subsequent MD simulations returned reasonable binding energies for the orientations clustered within 2 Å of the binding model shown in Fig. 8. All poses at this resolution reveal the macrolactone within the pocket defined by D295, A296, P305, R306, N337, and Y340, oriented such that the modified pyran group is deeply embedded. These amino acid residues are contained in peptides detected in the labelling experiment, indicating a good correlation. In this model, peloruside A appears to interact with Q291 on a helical segment (H9) leading into the pocket, where no overlap with labelling data is seen. This is likely due to the relative insensitivity of the helix as a reporter of binding, much as βH7 was for the taxoid-site ligands (Fig. 6).

While the region spanning the interdimer interface cannot be ruled out as a secondary binding site (Fig. 7c), it is less likely for four reasons. First, the labelling reductions observed in this region are also seen in both epothilone A and docetaxel-stabilized micro-

tubules, suggesting that this region represents improved dimer–dimer interactions (i.e., the T5 loop reductions discussed above). Second, in the case of peloruside, the labelling data offer a poor overlap with the ligand-docking results particularly as the largest reduction in deuterium labelling is fully within the interdimer interface (data not shown). Also, peptide α330–343 is within the site identified by localized docking; however, it does not show a decrease in labelling upon peloruside binding, even though it is a sensitive reporter of deuteration change (Fig. 2a). Third, MD simulations demonstrate higher binding energies than those generated at the primary site and, finally, the related compound laulimalide has been demonstrated to possess 1:1 binding stoichiometry with tubulin; thus, occupation of a second site is unlikely.

The binding site described in this work is at odds with recently published studies proposing a site centered at the M-loop of α-tubulin (α272–286)[37,45] in addition to partial occupation of the taxoid site.[45] Both studies utilized blind-docking procedures in AutoDock similar to the current study and refined their simulations around the α-tubulin site discovered in this fashion. A similar candidate site was found in the current study during blind docking, but as there was no significant reduction in labelling in this region, it was not considered in further simulations (see Fig. 9 for a comparison of proposed binding sites). Several of the residues proposed by Jimenez-Barbero *et al.*[37] that would be critical to stabilizing the peloruside A binding site on α-tubulin are located in regions that would be expected to show significant reductions in labelling upon binding, particularly the αH1 loop, the αS9–S10 loop, the αH7–H8 loop, and the αS8 loop. Reduced labelling is seen for peptide α352–368 (Fig. 2a) corresponding to the αS9–S10 loop, but the reduction is not significant. Furthermore, this peptide is only strongly affected by epothilone A; given that it also spans the interdimer interface, we interpret the reduction as arising from stabilization in this region. It remains possible that a translocation in this loop to expose the binding site (leading to an increase in labelling) is counterbalanced by the binding event itself (leading to a decrease in labelling). This is in fact suggested by Pineda *et al.*,[45] where the movement of this loop was required for lowest energy binding. However, it is difficult to see how binding at the α-tubulin site could rationalize the large reduction in labelling seen in the proposed β-tubulin site. Resolution of the conflicting models awaits further study.

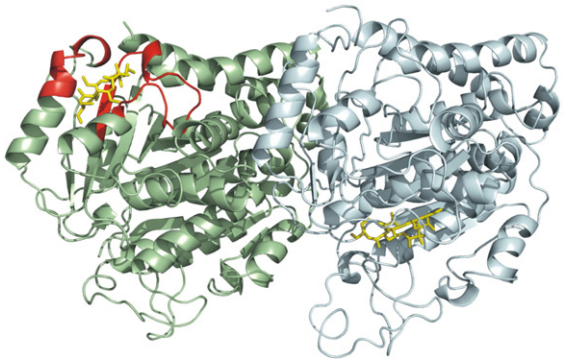

Fig. 9. Comparison between the data-directed docked pose of peloruside A (this study) and that proposed by Jimenez-Barbero *et al.*[37] This rendering depicts the interdimer interface between β-tubulin (pale green) from one dimer and α-tubulin (pale cyan) from an adjacent dimer. HDX data aligning with the docked pose of current study is displayed in red, and peloruside A in yellow.

In conclusion, it has been shown that stabilizing agents can affect overall stability of the microtubule through a mechanism primarily involving improved longitudinal contacts across the interdimer interface, and that improved lateral protofilament contacts may not be a requirement. Peloruside A ligation presents a significant mechanistic departure from the taxoid-site ligands, whereby a relaxation of the intradimer interface and β−β interaction across the lateral interface accompanies binding. Data-directed docking strongly suggests the identification of a novel stabilizer site on β-tubulin independent of the taxoid site, and a model is proposed that can be tested in mutational and lead optimization studies.

Materials and Methods

Microtubule preparation and labelling

Purified bovine brain tubulin (Cytoskeleton Inc., cat. no. TL238-A) was reconstituted in nucleotide-free buffer (20 mM KCl, 10 mM K-Pipes, pH 6.9) to 20 mg/ml and incubated at 37 °C for 30 min to initiate polymerization and hydrolysis of GTP present in storage buffer. The resulting microtubules were pelleted and washed with a small amount of assembly buffer (1 mM GMPCPP, 100 mM KCl, 10 mM K-Pipes, 1 mM $MgCl_2$, pH 6.9), then depolymerized on ice to a concentration of >60 μM. Prior to conducting HDX-MS experiments, an aliquot of this cold solution was incubated at 37 °C for 30 min to induce polymerization. The solution was brought to room temperature and labeled by addition of an equal volume of D_2O (50% labelling, to minimize the influence on D_2O assembly and dynamics seen at higher levels[46]). These exchange conditions were preserved for 4 min prior to quenching. Deuterium labelling experiments were conducted at several time points, and it was determined that dimer labelling was essentially complete after 4 min (data not shown). This period was used for all subsequent comparisons of assembled and drug-stabilized microtubule states. To prepare drug-saturated microtubules, the procedure was repeated with the addition of docetaxel (200 μM), peloruside (125 μM), or epothilone A (125 μM) to the assembly buffer. Docetaxel and epothilone A were purchased from Sigma-Aldrich and peloruside was synthesized as described elsewhere.[47]

The termination of labelling and the initiation of pepsin digestion was achieved by adding the labeled sample to a chilled slurry of immobilized pepsin (Applied Biosystems Inc.) in 0.1 M glycine–HCl (pH 2.3) and digesting for 2.5 min on ice. Digestion was terminated by centrifugation of the immobilized pepsin and an aliquot of the supernatant (containing ~30 pmol of digest) was injected into the LC-MS system for analysis. All analyses were performed in triplicate.

HDX LC-MS system

The LC-MS system consisted of an injection valve, a column loading pump, a prototype splitless low-flow gradient pump (Upchurch Scientific Inc.), and a QStar Pulsar *i* mass spectrometer (AB/Sciex Inc.) fitted with a turbo ion spray source. Chilled digest was injected onto a 150-μm ID×65-mm C18 column prepared in-house. The valve, column, and fluid lines were housed in a chilled container (~0 °C) to minimize the back-exchange of deuterium label during analysis. A rapid gradient separation was performed, and the total time for analysis (from digestion to analysis) was 16 min. The mass spectrometer was operated in positive polarity and time-of-flight MS mode (m/z range from 300 to 1200).

Peptide identification

Non-labeled tubulin was digested with pepsin as described and analyzed by LC-MS/MS at room temperature. MS/MS spectra were obtained via recursive information-dependent acquisitions and manual product ion acquisitions to maximize the number of peptides detected. Spectra were searched against a custom database assembled to capture the sequence diversity present in the mixture of bovine brain tubulin, using MASCOT. To create the database, porcine sequences for α- and β-tubulin (P02550 and P02554) were searched against the TIGR cattle EST database (v. 11.0) to generate a number of contigs. The same procedure was applied to the bovine Ensembl database (v. 37). A total of 31 contigs were compiled, to which was added the porcine sequences and recent bovine entries to the SwissProt database. Applying this workflow, 84 non-redundant peptides for α-tubulin (88.4% sequence coverage) and 86 non-redundant peptides for β-tubulin (92% sequence coverage) were identified. Sequencing results were manually verified.

Data analysis and presentation

Average deuterium incorporation for all verified peptide sequences was determined using software developed by our group. Standard deviations were determined from triplicate analyses of ligand-saturated and ligand-free microtubules on a per-peptide basis. A labelling difference between states for a given peptide is reported as significant if it passed two criteria: first, a two-tailed t test ($P<0.02$) using pooled standard deviations from the two triplicate analyses (pooling was deemed acceptable on the basis of per-peptide F-tests); second, a visual inspection of the isotopic distributions to guard against spectral overlap in conjunction with manual inspection of tandem MS data for peptide purity. Levels of ΔD were color coded per peptide on PDB entries 1JFF and 1TVK. Tubulin structures were rendered in all figures using Pymol†.

Molecular modeling—docking

Ligand docked was conducted with AutoDock 3‡. To perform the automated ligand-docking search, it was essential to obtain an accurate representation of the bound peloruside molecule, as AutoDock does not search torsions within ring structures. Following the construction of an initial peloruside model using the Prodrg server,[48] dihedral angles similar to those reported for the B-solvated conformer[37] were assigned using the Leap module of AMBER8.[49] The system was then optimized with Gaussian03, at the Hartree Fock level with a 6–31G(d,p) basis set, producing our final macrolide ring conformation. Following Quantum Mechanics optimization, we obtained the electrostatic potential fit charges using the Merz–Singh–Kollman method within Gaussian03. These charges were then entered into the AutoDock 3 implementation of the AMBER force field and the molecule imported into AutoDock.[50] The α and β chains of the 1TVK PDB file, without bound nucleotides or epothilone, were used to construct an α–β–α protofilament to act as the receptor for subsequent blind docking runs. The tubulin complex was then imported into AutoDock 3 and default Kollman's united atoms partial charges and solvent parameters were added.

In the blind docking exercise, the entire exterior surface of the α–β–α protofilament (i.e., inclusive of the interdimer interface) was interrogated using a grid box with a coarse spacing of 0.825 Å and dimensions of 126×62×72 points. Using the Lamarckian genetic algorithm, we performed 500 trials of 1×10^7 energy evaluations for each trial and docked poses were clustered using RMSD tolerances of 5 Å. In the refined docking study, we focused the search on the general area of the exterior of β-tubulin centered on the site indicated by the HDX data, and the interdimer region. A default grid spacing of 0.325 Å and box dimensions of 96×86×96 points were used in both cases. We then performed 200 trials of 1×10^7 energy evaluations each. Docked poses were clustered using RMSD tolerances of 2 Å.

Molecular modeling—molecular dynamics

After identification of the preferred binding site, peloruside was imported into AMBER8 and parameters were assigned using Antechamber and charges were obtained as above. Parameters for the tubulin dimer were taken from the AMBER99 force field. A short steepest descents/conjugate gradient minimization was performed, producing our minimized input structures for MD simulations. MD simulations were performed both *in vacuo* and using the generalized Born implicit solvation model. In both cases, the system was restrained and thermalized from 0 to 300 K over approximately 100 ps. Unrestrained MD was then performed for an additional nanosecond, after which binding energies were evaluated over the last three-quarters of each trajectory. Using MM-GBSA (Molecular Mechanics - Generalized Born Surface Area), we evaluated the binding energy using vacuum electrostatics and approximated solvation using the generalized Born model.

† http://pymol.sourceforge.net
‡ http://autodock.scripps.edu/

Acknowledgements

We acknowledge Tyler Luchko for assisting in the creation of the α–β–α protofilament from periodic images from the crystal structure of epothilone-bound tubulin. This work was supported by the Alberta Cancer Board, the Alberta Heritage Foundation for Medical Research, the Canadian Institutes of Health Research and intramural funds from the National Institute of Child Health and Human

Development, National Institutes of Health, USA. D.C.S. thanks the CRC for a Canada Research Chair.

Supplementary Data

Supplementary data associated with this article can be found, in the online version, at doi:10.1016/j.jmb.2008.03.026

References

1. Nettles, J. H., Li, H. L., Cornett, B., Krahn, J. M., Snyder, J. P. & Downing, K. H. (2004). The binding mode of epothilone A on alpha,beta-tubulin by electron crystallography. *Science*, **305**, 866–869.
2. Bergstralh, D. T. & Ting, J. P. (2006). Microtubule stabilizing agents: their molecular signaling consequences and the potential for enhancement by drug combination. *Cancer Treat. Rev.* **32**, 166–179.
3. Chao, T. C., Chu, Z., Tseng, L. M., Chiou, T. J., Hsieh, R. K., Wang, W. S. *et al.* (2005). Paclitaxel in a novel formulation containing less Cremophor EL as first-line therapy for advanced breast cancer: a phase II trial. *Invest New Drugs*, **23**, 171–177.
4. Weiss, R. B., Donehower, R. C., Wiernik, P. H., Ohnuma, T., Gralla, R. J., Trump, D. L. *et al.* (1990). Hypersensitivity reactions from taxol. *J. Clin. Oncol.* **8**, 1263–1268.
5. Gelderblom, H., Verweij, J., Nooter, K. & Sparreboom, A. (2001). Cremophor EL: the drawbacks and advantages of vehicle selection for drug formulation. *Eur. J. Cancer*, **37**, 1590–1598.
6. West, L. M., Northcote, P. T. & Battershill, C. N. (2000). Peloruside A: a potent cytotoxic macrolide isolated from the New Zealand marine sponge *Mycale* sp. *J. Org. Chem.* **65**, 445–449.
7. Mooberry, S. L., Tien, G., Hernandez, A. H., Plubrukarn, A. & Davidson, B. S. (1999). Laulimalide and isolaulimalide, new paclitaxel-like microtubule-stabilizing agents. *Cancer Res.* **59**, 653–660.
8. Hood, K. A., West, L. M., Rouwe, B., Northcote, P. T., Berridge, M. V., Wakefield, S. J. & Miller, J. H. (2002). Peloruside A, a novel antimitotic agent with paclitaxel-like microtubule-stabilizing activity. *Cancer Res.* **62**, 3356–3360.
9. Gaitanos, T. N., Buey, R. M., Diaz, J. F., Northcote, P. T., Teesdale-Spittle, P., Andreu, J. M. & Miller, J. H. (2004). Peloruside A does not bind to the taxoid site on beta-tubulin and retains its activity in multidrug-resistant cell lines. *Cancer Res.* **64**, 5063–5067.
10. Hamel, E., Day, B. W., Miller, J. H., Jung, M. K., Northcote, P. T., Ghosh, A. K. *et al.* (2006). Synergistic effects of peloruside A and laulimalide with taxoid site drugs, but not with each other, on tubulin assembly. *Mol. Pharmacol.* **70**, 1555–1564.
11. Gapud, E. J., Bai, R., Ghosh, A. K. & Hamel, E. (2004). Laulimalide and paclitaxel: a comparison of their effects on tubulin assembly and their synergistic action when present simultaneously. *Mol. Pharmacol.* **66**, 113–121.
12. Wilmes, A., Bargh, K., Kelly, C., Northcote, P. T. & Miller, J. H. (2007). Peloruside A synergizes with other microtubule stabilizing agents in cultured cancer cell lines. *Mol. Pharm.* **4**, 269–280.
13. Pryor, D. E., O'Brate, A., Bilcer, G., Diaz, J. F., Wang, Y., Wang, Y. *et al.* (2002). The microtubule stabilizing agent laulimalide does not bind in the taxoid site, kills cells resistant to paclitaxel and epothilones, and may not require its epoxide moiety for activity. *Biochemistry*, **41**, 9109–9115.
14. Diaz, J. F., Valpuesta, J. M., Chacon, P., Diakun, G. & Andreu, J. M. (1998). Changes in microtubule protofilament number induced by Taxol binding to an easily accessible site. Internal microtubule dynamics. *J. Biol. Chem.* **273**, 33803–33810.
15. Wade, R. H., Chretien, D. & Job, D. (1990). Characterization of microtubule protofilament numbers. How does the surface lattice accommodate? *J. Mol. Biol.* **212**, 775–786.
16. Desai, A. & Mitchison, T. J. (1997). Microtubule polymerization dynamics. *Annu. Rev. Cell. Dev. Biol.* **13**, 83–117.
17. Wang, H. W. & Nogales, E. (2005). Nucleotide-dependent bending flexibility of tubulin regulates microtubule assembly. *Nature*, **435**, 911–915.
18. Löwe, J., Li, H., Downing, K. H. & Nogales, E. (2001). Refined structure of alpha beta-tubulin at 3.5 Å resolution. *J. Mol. Biol.* **313**, 1045–1057.
19. Thepchatri, P., Cicero, D. O., Monteagudo, E., Ghosh, A. K., Cornett, B., Weeks, E. R. & Snyder, J. P. (2005). Conformations of laulimalide in DMSO-d_6. *J. Am. Chem. Soc.* **127**, 12838–12846.
20. Maier, C. S. & Deinzer, M. L. (2005). Protein conformations, interactions, and H/D exchange. *Methods Enzymol.* **402**, 312–360.
21. Chik, J. K. & Schriemer, D. C. (2003). Hydrogen/deuterium exchange mass spectrometry of actin in various biochemical contexts. *J. Mol. Biol.* **334**, 373–385.
22. Xiao, H., Verdier-Pinard, P., Fernandez-Fuentes, N., Burd, B., Angeletti, R., Fiser, A., Horwitz, S. B. & Orr, G. A. (2006). Insights into the mechanism of microtubule stabilization by Taxol. *Proc. Natl. Acad. Sci. USA*, **103**, 10166–10173.
23. Maity, H., Lim, W. K., Rumbley, J. N. & Englander, S. W. (2003). Protein hydrogen exchange mechanism: local fluctuations. *Protein Sci.* **12**, 153–160.
24. Williams, D. H., Stephens, E., O'Brien, D. P. & Zhou, M. (2004). Understanding noncovalent interactions: ligand binding energy and catalytic efficiency from ligand-induced reductions in motion within receptors and enzymes. *Angew. Chem., Int. Ed.* **43**, 6596–6616.
25. Chalmers, M. J., Busby, S. A., Pascal, B. D., He, Y. J., Hendrickson, C. L., Marshall, A. G. & Griffin, P. R. (2006). Probing protein ligand interactions by automated hydrogen/deuterium exchange mass spectrometry. *Anal. Chem.* **78**, 1005–1014.
26. Hamuro, Y., Coales, S. J., Morrow, J. A., Molnar, K. S., Tuske, S. J., Southern, M. R. & Griffin, P. R. (2006). Hydrogen/deuterium-exchange (H/D-Ex) of PPAR gamma LBD in the presence of various modulators. *Protein Sci.* **15**, 1883–1892.
27. Anand, G. S., Law, D., Mandell, J. G., Snead, A. N., Tsigelny, I., Taylor, S. S. *et al.* (2003). Identification of the protein kinase A regulatory RIalpha-catalytic subunit interface by amide H/2H exchange and protein docking. *Proc. Natl. Acad. Sci. USA*, **100**, 13264–13269.
28. Banerjee, A., Roach, M. C., Trcka, P. & Luduena, R. F. (1992). Preparation of a monoclonal antibody specific for the class IV isotype of beta-tubulin. Purification and assembly of alpha beta II, alpha beta III, and alpha beta IV tubulin dimers from bovine brain. *J. Biol. Chem.* **267**, 5625–5630.
29. Derry, W. B., Wilson, L., Khan, I. A., Luduena, R. F. & Jordan, M. A. (1997). Taxol differentially modulates

the dynamics of microtubules assembled from unfractionated and purified beta-tubulin isotypes. *Biochemistry*, **36**, 3554–3562.
30. Diaz, J. F. & Andreu, J. M. (1993). Assembly of purified GDP-tubulin into microtubules induced by taxol and taxotere: reversibility, ligand stoichiometry, and competition. *Biochemistry*, **32**, 2747–2755.
31. Hyman, A. A., Salser, S., Drechsel, D. N., Unwin, N. & Mitchison, T. J. (1992). Role of GTP hydrolysis in microtubule dynamics: information from a slowly hydrolyzable analogue, GMPCPP. *Mol. Biol. Cell*, **3**, 1155–1167.
32. Wang, H. W., Long, S., Finley, K. R. & Nogales, E. (2005). Assembly of GMPCPP-bound tubulin into helical ribbons and tubes and effect of colchicine. *Cell Cycle*, **4**, 1157–1160.
33. Krishna, M. M., Hoang, L., Lin, Y. & Englander, S. W. (2004). Hydrogen exchange methods to study protein folding. *Methods*, **34**, 51–64.
34. Ehring, H. (1999). Hydrogen exchange electrospray ionization mass spectrometry studies of structural features of proteins and protein/protein interactions. *Anal. Biochem.* **267**, 252–259.
35. Buey, R. M., Barasoain, I., Jackson, E., Meyer, A., Giannakakou, P., Paterson, I. *et al.* (2005). Microtubule interactions with chemically diverse stabilizing agents: thermodynamics of binding to the paclitaxel site predicts cytotoxicity. *Chem. Biol.* **12**, 1269–1279.
36. Nogales, E., Whittaker, M., Milligan, R. A. & Downing, K. H. (1999). High-resolution model of the microtubule. *Cell*, **96**, 79–88.
37. Jimenez-Barbero, J., Canales, A., Northcote, P. T., Buey, R. M., Andreu, J. M. & Diaz, J. F. (2006). NMR determination of the bioactive conformation of peloruside A bound to microtubules. *J. Am. Chem. Soc.* **128**, 8757–8765.
38. Magnani, M., Ortuso, F., Soro, S., Alcaro, S., Tramontano, A. & Botta, M. (2006). The betaI/betaIII-tubulin isoforms and their complexes with antimitotic agents. Docking and molecular dynamics studies. *FEBS J.* **273**, 3301–3310.
39. Reese, M., Sanchez-Pedregal, V. M., Kubicek, K., Meiler, J., Blommers, M. J., Griesinger, C. & Carlomagno, T. (2007). Structural basis of the activity of the microtubule-stabilizing agent epothilone A studied by NMR spectroscopy in solution. *Angew. Chem., Int. Ed. Engl.* **46**, 1864–1868.
40. Correia, J. J. & Lobert, S. (2001). Physiochemical aspects of tubulin-interacting antimitotic drugs. *Curr. Pharm. Des.* **7**, 1213–1228.
41. Nogales, E. & Wang, H. W. (2006). Structural mechanisms underlying nucleotide-dependent self-assembly of tubulin and its relatives. *Curr. Opin. Struct. Biol.* **16**, 221–229.
42. He, L. F., Yang, C. P. H. & Horwitz, S. B. (2001). Mutations in beta-tubulin map to domains involved in regulation of microtubule stability in epothilone-resistant cell lines. *Mol. Cancer Ther.* **1**, 3–10.
43. Laederach, A., Dowd, M. K., Coutinho, P. M. & Reilly, P. J. (1999). Automated docking of maltose, 2-deoxymaltose, and maltotetraose into the soybean beta-amylase active site. *Proteins: Struct., Funct., Genet.* **37**, 166–175.
44. Hetenyi, C. & van der Spoel, D. (2006). Blind docking of drug-sized compounds to proteins with up to a thousand residues. *FEBS Lett.* **580**, 1447–1450.
45. Pineda, O., Farras, J., Maccari, L., Manetti, F., Botta, M. & Vilarrasa, J. (2004). Computational comparison of microtubule-stabilising agents laulimalide and peloruside with taxol and colchicine. *Bioorg. Med. Chem. Lett.* **14**, 4825–4829.
46. Panda, D., Chakrabarti, G., Hudson, J., Pigg, K., Miller, H. P., Wilson, L. & Himes, R. H. (2000). Suppression of microtubule dynamic instability and treadmilling by deuterium oxide. *Biochemistry*, **39**, 5075–5081.
47. Jin, M. & Taylor, R. E. (2005). Total synthesis of (+)-peloruside A. *Org. Lett.* **7**, 1303–1305.
48. Schuttelkopf, A. W. & van Aalten, D. M. F. (2004). PRODRG: a tool for high-throughput crystallography of protein–ligand complexes. *Acta Crystallogr., Sect. D: Biol. Crystallogr.* **60**, 1355–1363.
49. Case, D. A., Cheatham, T. E., 3rd, Darden, T., Gohlke, H., Luo, R., Merz, K. M., Jr. *et al.* (2005). The Amber biomolecular simulation programs. *J. Comput. Chem.* **26**, 1668–1688.
50. Morris, G. M., Goodsell, D. S., Halliday, R. S., Huey, R., Hart, W. E., Belew, R. K. & Olson, A. J. (1998). Automated docking using a Lamarckian genetic algorithm and an empirical binding free energy function. *J. Comput. Chem.* **19**, 1639–1662.